



Edge Functionalization of Structurally Defined Graphene Nanoribbons for Modulating the Self-Assembled Structures

Ashok Keerthi,^{†,§,‡,†} Boya Radha,^{§,‡} Daniele Rizzo,[#] Hao Lu,[†] Valentin Diez Cabanes,^{||} Ian Cheng-Yi Hou,[†] David Beljonne,^{||} Jérôme Cornil,^{||} Cinzia Casiraghi,[#] Martin Baumgarten,^{†,†} Klaus Müllen,^{*,†,†} and Akimitsu Narita^{*,†,†}

[†]Max Planck Institute for Polymer Research, Ackermannweg 10, 55128 Mainz, Germany

[§]National Graphene Institute, University of Manchester, Booth Street East, Manchester M13 9PL, United Kingdom

[‡]School of Physics and Astronomy, University of Manchester, Oxford Road, Manchester M13 9PL, United Kingdom

[#]School of Chemistry, University of Manchester, Oxford Road, Manchester M13 9PL, United Kingdom

^{||}Laboratory for Chemistry of Novel Materials, University of Mons, Place du Parc 20, B-7000 Mons, Belgium

Supporting Information

ABSTRACT: Edge functionalization of bottom-up synthesized graphene nanoribbons (GNRs) with anthraquinone and naphthalene/peryene monoimide units has been achieved through a Suzuki coupling of polyphenylene precursors bearing bromo groups, prior to the intramolecular oxidative cyclo-dehydrogenation. High efficiency of the substitution has been validated by MALDI-TOF MS analysis of the functionalized precursors and FT-IR, Raman, and XPS analyses of the resulting GNRs. Moreover, AFM measurements demonstrated the modulation of the self-assembling behavior of the edge-functionalized GNRs, revealing that GNR-PMI formed an intriguing rectangular network. This result suggests the possibility of programming the supramolecular architecture of GNRs by tuning the functional units.

Bottom-up molecular synthesis of graphene nanoribbons (GNRs), namely nanometer-wide graphene strips, has been attracting growing attention for its high capability of fabricating atomically precise GNR structures with promising electronic, optical, and magnetic properties.^{1–10} In particular, GNRs have non-zero bandgap, which can be tuned by changing their structures, in stark contrast to zero-bandgap graphene.^{1,11} While the top-down methods such as “cutting” of graphene¹² and “unzipping” of carbon nanotubes¹³ can only provide rather undefined and randomly shaped GNRs, uniform and highly defined GNRs can be obtained through the oxidative cyclo-dehydrogenation of tailor-made polyarylene precursors, either in solution by the Scholl reaction^{4,5,14,15} or thermally on metal surfaces.^{2,3,7–9} In particular, a solution synthesis based on the AB-type Diels–Alder polymerization has enabled the preparation of exceptionally long (up to >600 nm) GNRs with tunable width (ca. 1–2 nm) and optical bandgaps (ca. 1.2–1.9 eV).^{14–18} Such GNRs are dispersible in organic solvents, and thus can be characterized in and processed from a liquid phase.

Peripheral functionalization of organic compounds is tremendously important in the field of organic materials for largely altering as well as fine-tuning their electronic, optical, and mechanical properties for various applications.¹⁹ Moreover,

appropriate pendant groups incorporated in supramolecular networks or polymers can pre-program their assembly into desired architectures.²⁰ Due to their 1D character, bottom-up GNRs can be viewed as a special class of organic polymers, where edge substitution allows further modulation of the properties, partly through changes in the supramolecular organization. Except for the conventional alkyl substitution, however, there are thus far only a few examples for such edge functionalization of GNRs, namely peripheral chlorination²¹ and introduction of carboxylic acid or nitronyl nitroxide (NN) radicals.^{22–24}

Here we report a versatile protocol to functionalize the GNR edges with different groups, through Suzuki coupling prior to the cyclo-dehydrogenation. We demonstrate successful introduction of anthraquinone (AQ), naphthalene monoimide (NMI), and perylene monoimide (PMI) units at the peripheral positions, which reveals an unprecedented effect on the self-assembly behavior of the GNRs.

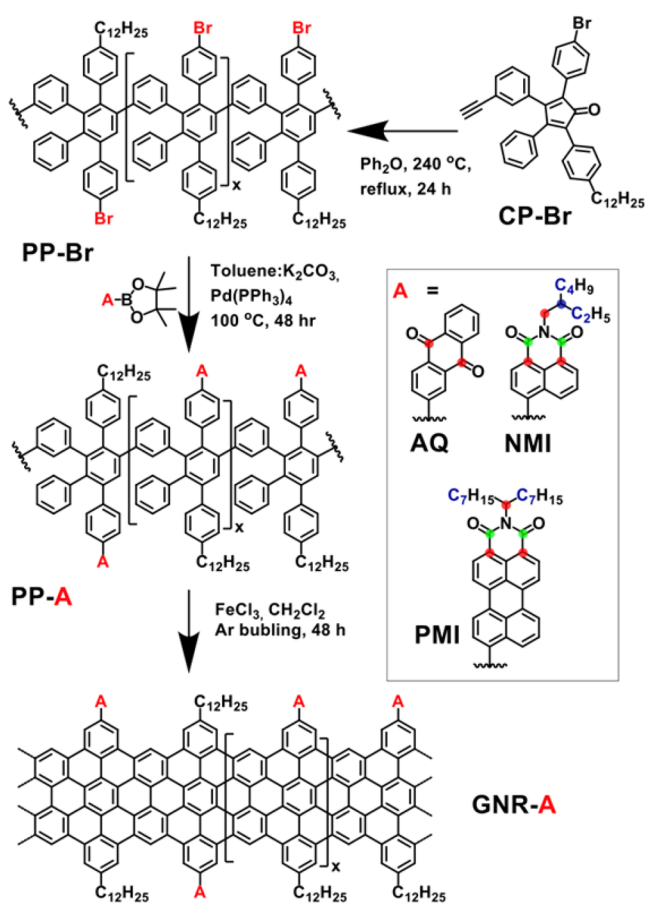
For the synthesis of GNRs appended with NN radicals, we have recently developed a polyphenylene precursor bearing one bromo group and one dodecyl chain per repeating unit (PP-Br), through the AB-type Diels–Alder polymerization of tetraphenylcyclopentadienone-based monomer CP-Br (Scheme 1).²⁴ Nevertheless, the method used for introducing the NN radical, mediated by an Au complex, is not immediately applicable to other functional groups, which motivated us to consider the use of more versatile Suzuki coupling. To this end, we have previously carried out a model study on the peripheral functionalization of hexa-*peri*-hexabenzocoronene (HBC) through the Suzuki coupling both before and after the cyclo-dehydrogenation, with boronic esters of AQ, NMI, and PMI.²⁵ Such electron-deficient groups were selected in the hope that it would yield less-explored n-type GNR materials, as actually supported by density functional theory (DFT) calculations. For example, substitution with the NMI or PMI unit is predicted to lower the energy levels of the GNR by 0.4–0.5 eV (see Supporting Information (SI) for the theoretical results).

Received: August 23, 2017

Published: November 3, 2017



Scheme 1. Synthetic Protocol for the Edge-Functionalization of GNRs with AQ, NMI, and PMI Units



Based on the successful results with HBC, PP-Br was thus subjected to the Suzuki coupling with three boronic esters, 2-(4,4,5,5-tetramethyl-1,3,2-dioxaborolan-2-yl)anthracene-9,10-dione (AQ-BPin), *N*-(2-ethylhexyl)-4-(4,4,5,5-tetramethyl-1,3,2-dioxaborolan-2-yl)naphthalene-1,8-dicarboximide (NMI-BPin), and *N*-(1-heptyloctyl)-9-(4,4,5,5-tetramethyl-1,3,2-dioxaborolan-2-yl)perylene-3,4-dicarboximide (PMI-BPin), using tetrakis(triphenylphosphine)palladium as catalyst and 2-dicyclohexylphosphino-2',6'-dimethoxybiphenyl (SPhos) as ligand, in a mixture of toluene, ethanol, and 1 M aqueous solution of K₂CO₃ (Scheme 1). After extensive purification and removal of small-molecular-weight fractions by reprecipitation, and also with recycling preparative size exclusion chromatography (SEC) when possible (see SI), functionalized polyphenylenes PP-A (A = AQ, NMI, and PMI) were obtained (Table S1).

Matrix-assisted laser desorption/ionization time-of-flight (MALDI-TOF) mass spectrometry (MS) analysis (in reflectron mode) of a low-molecular-weight fraction of PP-AQ has demonstrated a series of peaks from oligomers with up to 14 repeating units (Figure 1). The *m/z* and intervals were consistent with the expected values. The isotopic distributions were also generally in agreement with the simulated patterns, as displayed for the pentamers in the insets of Figure 1, validating the successful functionalization of the polyphenylene precursors with the AQ units. Notably, the MS spectrum showed no peak corresponding to PP-Br or partially substituted or debrominated oligomers, pointing to the high efficiency of the functionalization. Although the MALDI-TOF MS analysis of PP-NMI and -PMI was more difficult presumably due to stronger aggregation,

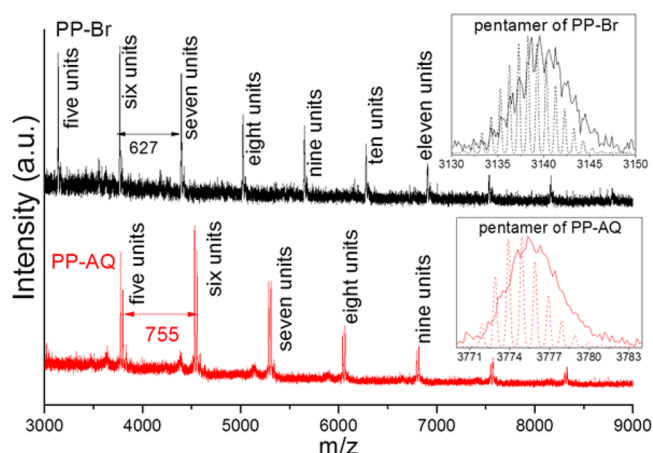


Figure 1. MALDI-TOF spectra of PP-Br and PP-AQ. Peaks with added sodium ion are also visible.¹⁴ Inset: calculated (dashed line) and observed (solid line) isotopic distribution of the pentamers.

expected patterns of mass could be observed for an oligomeric mixture of PP-NMI in the linear mode (Figure S4). NMR of the three PP-A could not be properly measured even at 120 °C in C₂D₂Cl₄, probably also due to the aggregation, but the MS results combined with the observation of characteristic IR peaks (Figures S6–S8) indicated successful introduction of the functional groups.

The three PP-A were subsequently “graphitized” into GNR-A (A = AQ, NMI, and PMI), through the oxidative cyclo-dehydrogenation using FeCl₃ in dichloromethane and nitromethane, following the literature protocol.^{14,25} It must be noted that PP-Br, and thus also PP-A were obtained as mixtures of regioisomers because of two possible orientations of the unsymmetrical CP-Br on each Diels–Alder cycloaddition step. However, all the regioisomers of PP-A could lead to GNR-A with the uniform GNR core structure,¹⁴ although having a statistical distribution for the orientation of the dodecyl and the other pendant groups (Scheme S1). According to the previous model study with HBC, the AQ, NMI, and PMI units used here are chemically stable under the oxidative cyclo-dehydrogenation condition with FeCl₃ and form no extra C–C bond with the aromatic core, which would potentially make a five-membered ring.²⁵ To explore the possibility of the post-functionalization of the GNRs, we also attempted a synthesis of GNR-PMI through the prior cyclo-dehydrogenation of PP-Br to GNR-Br (Figure S1), followed by the Suzuki coupling with PMI-BPin (named as GNR-PMI*, Scheme S4). All the three functionalized GNRs, GNR-AQ, -NMI and -PMI could be dispersed in organic solvents such as tetrahydrofuran (THF), chlorobenzene, 1,2,4-trichlorobenzene (TCB), and 1,4-dioxane (see SI).

These GNRs were initially characterized by Fourier transform infrared (FT-IR) and Raman spectroscopy (Figures 2c and S5–S10). FT-IR analysis revealed the successful cyclo-dehydrogenation of the polyphenylene backbones to GNR core structures, displaying a clear disappearance/attenuation of out-of-plane (*opla*) C–H deformation bands at around 698 and 795 cm^{−1} (Figures S5–S8).¹⁴ Evidences for the functionalization of the GNRs could be obtained by the observation of C=O stretching bands, which are absent in the GNR core, at 1672 cm^{−1} for GNR-AQ, at 1660 and 1703 cm^{−1} for GNR-NMI, and at 1653 and 1691 cm^{−1} for GNR-PMI (Figure S5).²⁶ On the other hand, GNR-PMI* displayed a spectrum overall resembling that of GNR-Br, rather than that of GNR-PMI, with additional bands of

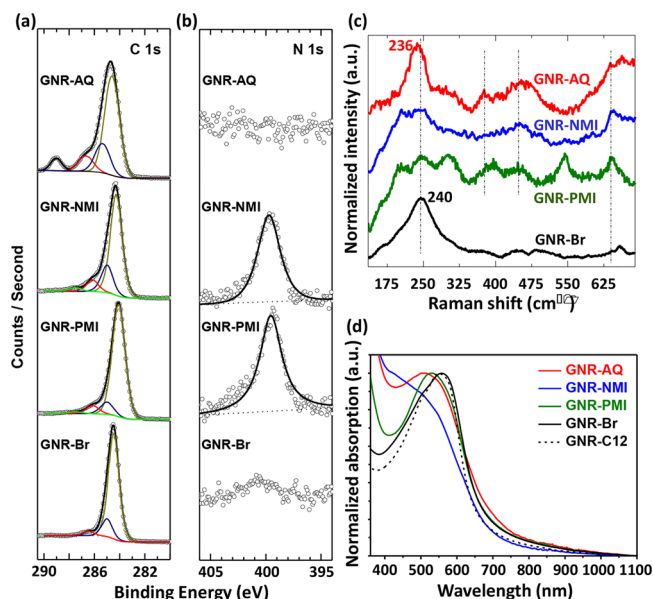


Figure 2. (a) C 1s and (b) N 1s XPS (circles, raw data; black, fitted curve for C 1s spectra: dark yellow, sp^2 ; navy blue, sp^3 ; red, sp^2 at C–Br for GNR-Br; see the color code in Scheme 1 for other GNRs). (c) Magnified Raman spectra in the low-energy region (at 2.33 eV). (d) Normalized UV–vis–NIR absorption spectra in NMP of the functionalized GNRs.

PMI units (Figure S9). This result most probably indicates that the post-functionalization after the cyclo-dehydrogenation is not as efficient as the pre-functionalization.

Raman spectra of GNR-AQ, -NMI, and -PMI show the first-order D and G as well as the second-order 2D, D+D', and 2D' peaks, which are generally in agreement with the spectra of GNR-Br and previous solution-synthesized GNRs,^{14,15,27} without significant changes upon the functionalization with different groups (Figure S10). In contrast, characteristic peaks in the low-energy regions, as represented by the radial-like breathing mode (RLBM) dependent on the GNR width,^{28,29} change significantly (Figure 2c). GNR-Br displayed a prominent RLBM peak at about 240 cm^{-1} , in close agreement with that of the same GNR substituted only with dodecyl chains (GNR-C12) observed at about 230 cm^{-1} .²⁷ A RLBM peak at $\sim 236\text{ cm}^{-1}$ was still visible for GNR-AQ, but no clear peak could be unambiguously assigned to the RLBM for GNR-PMI and -NMI, which could be related to the size of the pendant units: relatively large functional groups, such as PMI, seem to affect the RLBM,²⁷ either by decreasing its vibrational frequency below the cut of the edge filter or by quenching the vibrational mode by inducing structural deformation of the GNR core. Additionally, a prominent RLBM peak was observed for GNR-PMI*, like that of GNR-Br (Figure S11). This result suggests the low efficiency of the post-functionalization in agreement with FT-IR results, and simultaneously verifies that the RLBM peak was “quenched” by the covalently bonded PMI units.

Further evidence of functionalization could be obtained by X-ray photoelectron spectroscopy (XPS) analysis (Figure 2a,b). C 1s high resolution spectra displayed slight shift of the sp^2 binding energy from GNR-Br (284.5 eV) to GNR-NMI (284.3 eV), and then to GNR-PMI (284.1 eV), which is most probably the effect of the varying functional groups attached to the aromatic GNR core. Moreover, C 1s peaks assignable to the imide carbon (marked with light green in Scheme 1) could be observed

together with N 1s peaks for GNR-NMI and -PMI, and not for GNR-Br and -AQ. Based on the N/C ratios, the degree of functionalization could be estimated for GNR-NMI and -PMI to be 90 ± 16 and $91 \pm 24\%$, respectively (see SI for more details).

UV–vis–near-infrared (NIR) absorption spectra of GNR-PMI in NMP displayed absorption maximum at 530 nm with a shoulder peak at ~ 560 nm, which coincide with the absorption maxima of GNR-Br and -C12 and presumably correspond to the optical transition of the GNR core (Figure 2d). GNR-PMI* from the attempted post-functionalization also showed a maximum at 530 nm, indicating that this was not derived from partially fused GNRs, but rather from the PMI units (Figure S14). Although with broadening, the absorption spectra of GNR-Br, -AQ, and -PMI are weakly affected by the edge substitution, in line with the theoretical calculations (see SI for details). GNR-NMI exhibited rather broadened absorption, but with a shoulder peak at ~ 560 nm, consistent with other GNRs studied here. The absorption at around 400–500 nm might be from the NMI units, red-shifted due to aggregation and/or interaction with neighboring GNR, although the possibility of “defects” cannot be excluded.

In order to study the self-assembly behavior of the functionalized GNRs, their dispersions in TCB were drop-cast over freshly peeled graphite surfaces. AFM imaging revealed that GNR-AQ and -NMI can form closely packed assembly (Figures 3a,c and S19) similar to our previous observations with GNR-

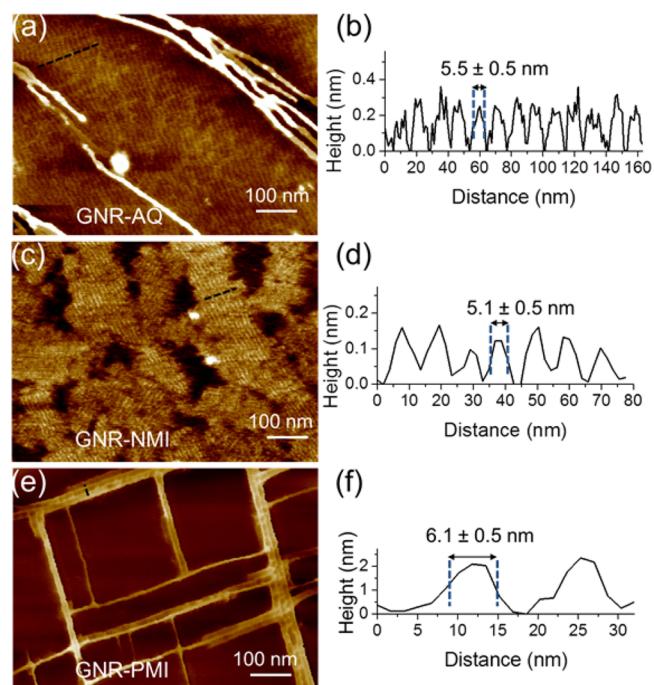


Figure 3. AFM height image of functionalized GNRs drop-cast on graphite in TCB solvent and annealed at $100\text{ }^\circ\text{C}$ demonstrates highly organized self-assembled monolayers of straight and uniform nanoribbons.

C12.¹⁴ In contrast, the deposition of the GNR-PMI in the same way reproducibly provided self-assembled rectangular networks, where single strands or bundles of GNRs crossed perpendicularly to each other (Figures 3e, S19, and S20). The widths observed for the ribbons are GNR-PMI (6.1 nm) > GNR-NMI (5.1 nm), in agreement with the simulated values (Figures S21 and S22). GNR-PMI showed a length of up to $1\text{ }\mu\text{m}$, although it could be

due to an end-to-end overlap of individual GNRs, or alignment of a few GNRs to form such supramolecular wires. The intriguing rectangular assembly of GNR-PMI might be due to the additional π - π interactions between the GNR cores and the PMI units, which are perpendicularly connected to the GNRs (Figure S23). The absence of such assembly with the NMI units indicates that extending the aromatic core of the pendant units can modulate the supramolecular architecture of the GNRs in such a drastic manner. Furthermore, isolated individual strand of GNR-PMI could be readily found under AFM analysis, which is an important step forward toward the application of the GNRs in the future nanoelectronics.

In summary, we have demonstrated successful edge functionalization of GNRs, based on the Suzuki coupling prior to the cyclo-dehydrogenation, which could be evidenced by a combination of MS and different spectroscopic characterizations. Notably, GNR-PMI revealed unprecedented self-assembly behavior, leading to rectangular network of GNRs. These results indicate the possibility of arbitrarily programming the self-assembled architectures of GNRs by the edge functionalization with proper pendent groups.

■ ASSOCIATED CONTENT

Supporting Information

The Supporting Information is available free of charge on the ACS Publications website at DOI: 10.1021/jacs.7b09031.

Materials and methods, syntheses, spectra, properties, characterization data, and structures, including Figures S1–S23 and Tables S1–S5 (PDF)

■ AUTHOR INFORMATION

Corresponding Authors

*muellen@mpip-mainz.mpg.de

*narita@mpip-mainz.mpg.de

ORCID

Ashok Keerthi: 0000-0002-8479-4762

Martin Baumgarten: 0000-0002-9564-4559

Klaus Müllen: 0000-0001-6630-8786

Akimitsu Narita: 0000-0002-3625-522X

Notes

The authors declare no competing financial interest.

■ ACKNOWLEDGMENTS

We are grateful for financial support from the Max Planck Society, the ERC grants on NANOGRAPH and 2DNOG (GA No. 648417), EC through the Graphene Flagship, iSwitch (GA No. 642196), and MoQuaS (FP7 FET-ICT-2013-10 610449), and the Office of Naval Research BRC Program. A.K. would like to thank Xinliang Feng (TU Dresden) for discussion and support. B.R. is thankful to Leverhulme trust for early career fellowship. D.R. acknowledges the EPSRC in the framework of a DTA studentship.

■ REFERENCES

- (1) Narita, A.; Wang, X.-Y.; Feng, X.; Müllen, K. *Chem. Soc. Rev.* **2015**, *44*, 6616.
- (2) Ruffieux, P.; Wang, S.; Yang, B.; Sánchez-Sánchez, C.; Liu, J.; Dienel, T.; Talirz, L.; Shinde, P.; Pignedoli, C. A.; Passerone, D.; Dumslaff, T.; Feng, X.; Müllen, K.; Fasel, R. *Nature* **2016**, *531*, 489.
- (3) Chen, Y.-C.; Cao, T.; Chen, C.; Pedramrazi, Z.; Haberler, D.; de Oteyza, D. G.; Fischer, F. R.; Louie, S. G.; Crommie, M. F. *Nat. Nanotechnol.* **2015**, *10*, 156.

- (4) Vo, T. H.; Shekhirev, M.; Kunkel, D. A.; Morton, M. D.; Berglund, E.; Kong, L.; Wilson, P. M.; Dowben, P. A.; Enders, A.; Sinititskii, A. *Nat. Commun.* **2014**, *5*, 3189.
- (5) Gao, J.; Uribe-Romo, F. J.; Saathoff, J. D.; Arslan, H.; Crick, C. R.; Hein, S. J.; Itin, B.; Clancy, P.; Dichtel, W. R.; Loo, Y.-L. *ACS Nano* **2016**, *10*, 4847.
- (6) Jordan, R. S.; Wang, Y.; McCurdy, R. D.; Yeung, M. T.; Marsh, K. L.; Khan, S. I.; Kaner, R. B.; Rubin, Y. *Chem* **2016**, *1*, 78.
- (7) de Oteyza, D. G.; Garcia-Lekue, A.; Vilas-Varela, M.; Merino-Diez, N.; Carbonell-Sanroma, E.; Corso, M.; Vasseur, G.; Rogero, C.; Guitian, E.; Pascual, J. I.; Ortega, J. E.; Wakayama, Y.; Pena, D. *ACS Nano* **2016**, *10*, 9000.
- (8) Talirz, L.; Ruffieux, P.; Fasel, R. *Adv. Mater.* **2016**, *28*, 6222.
- (9) Sakaguchi, H.; Song, S.; Kojima, T.; Nakae, T. *Nat. Chem.* **2017**, *9*, 57.
- (10) Kawai, S.; Saito, S.; Osumi, S.; Yamaguchi, S.; Foster, A. S.; Spijker, P.; Meyer, E. *Nat. Commun.* **2015**, *6*, 8098.
- (11) Ye, R.; Xiang, C.; Lin, J.; Peng, Z.; Huang, K.; Yan, Z.; Cook, N. P.; Samuel, E. L. G.; Hwang, C.-C.; Ruan, G.; Ciriotti, G.; Raji, A.-R. O.; Marti, A. A.; Tour, J. M. *Nat. Commun.* **2013**, *4*, 2943.
- (12) Chen, Z.; Lin, Y.-M.; Rooks, M. J.; Avouris, P. *Phys. E* **2007**, *40*, 228.
- (13) Kosynkin, D. V.; Higginbotham, A. L.; Sinititskii, A.; Lomeda, J. R.; Dimiev, A.; Price, B. K.; Tour, J. M. *Nature* **2009**, *458*, 872.
- (14) Narita, A.; Feng, X.; Hernandez, Y.; Jensen, S. A.; Bonn, M.; Yang, H.; Verzhbitskiy, I. A.; Casiraghi, C.; Hansen, M. R.; Koch, A. H. R.; Fytas, G.; Ivasenko, O.; Li, B.; Mali, K. S.; Balandina, T.; Mahesh, S.; De Feyter, S.; Müllen, K. *Nat. Chem.* **2014**, *6*, 126.
- (15) Narita, A.; Verzhbitskiy, I. A.; Frederickx, W.; Mali, K. S.; Jensen, S. A.; Hansen, M. R.; Bonn, M.; De Feyter, S.; Casiraghi, C.; Feng, X.; Müllen, K. *ACS Nano* **2014**, *8*, 11622.
- (16) Zhao, S.; Rondin, L.; Delport, G.; Voisin, C.; Beser, U.; Hu, Y.; Feng, X.; Müllen, K.; Narita, A.; Campidelli, S.; Lauret, J. S. *Carbon* **2017**, *119*, 235.
- (17) Ivanov, I.; Hu, Y.; Osella, S.; Beser, U.; Wang, H. I.; Beljonne, D.; Narita, A.; Müllen, K.; Turchinovich, D.; Bonn, M. *J. Am. Chem. Soc.* **2017**, *139*, 7982.
- (18) Soavi, G.; Dal Conte, S.; Manzoni, C.; Viola, D.; Narita, A.; Hu, Y.; Feng, X.; Hohenester, U.; Molinari, E.; Prezzi, D.; Müllen, K.; Cerullo, G. *Nat. Commun.* **2016**, *7*, 11010.
- (19) Wu, Z. S.; Parvez, K.; Feng, X.; Müllen, K. *Nat. Commun.* **2013**, *4*, 2487.
- (20) Baumgartner, R.; Fu, H.; Song, Z.; Lin, Y.; Cheng, J. *Nat. Chem.* **2017**, *9*, 614.
- (21) Tan, Y.-Z.; Yang, B.; Parvez, K.; Narita, A.; Osella, S.; Beljonne, D.; Feng, X.; Müllen, K. *Nat. Commun.* **2013**, *4*, 2646.
- (22) Rogers, C.; Perkins, W. S.; Veber, G.; Williams, T. E.; Cloke, R. R.; Fischer, F. R. *J. Am. Chem. Soc.* **2017**, *139*, 4052.
- (23) Huang, Y.; Mai, Y.; Beser, U.; Teyssandier, J.; Velpula, G.; van Gorp, H.; Straasø, L. A.; Hansen, M. R.; Rizzo, D.; Casiraghi, C.; Yang, R.; Zhang, G.; Wu, D.; Zhang, F.; Yan, D.; De Feyter, S.; Müllen, K.; Feng, X. *J. Am. Chem. Soc.* **2016**, *138*, 10136.
- (24) Slota, M.; Keerthi, A.; Myers, W. K.; Tretyakov, E.; Baumgarten, M.; Ardavan, A.; Sadeghi, H.; Lambert, C. J.; Narita, A.; Müllen, K.; Bogani, L. *Nature* **2017**, in press.
- (25) Keerthi, A.; Hou, I. C.; Marszalek, T.; Pisula, W.; Baumgarten, M.; Narita, A. *Chem. - Asian J.* **2016**, *11*, 2710.
- (26) Nagao, Y.; Misono, T. *Bull. Chem. Soc. Jpn.* **1981**, *54*, 1575.
- (27) Verzhbitskiy, I. A.; Corato, M. D.; Ruini, A.; Molinari, E.; Narita, A.; Hu, Y.; Schwab, M. G.; Bruna, M.; Yoon, D.; Milana, S.; Feng, X.; Müllen, K.; Ferrari, A. C.; Casiraghi, C.; Prezzi, D. *Nano Lett.* **2016**, *16*, 3442.
- (28) Guo, Z.; Zhang, D.; Gong, X.-G. *Appl. Phys. Lett.* **2009**, *95*, 163103.
- (29) Gillen, R.; Mohr, M.; Maultzsch, J. *Phys. Rev. B: Condens. Matter Mater. Phys.* **2010**, *81*, 205426.